

Multi-color image compression-encryption algorithm based on chaotic system and fuzzy transform

M. Zarebnia^{a*}, R. Kianfar^{a†}, R. Parvaz^{a‡}

^aDepartment of Mathematics, University of Mohaghegh Ardabili, 56199-11367
Ardabil, Iran.

Abstract

In this paper an algorithm for multi-color image compression-encryption is introduced. For compression step fuzzy transform based on exponential b-spline function is used. In encryption step, a novel combination chaotic system based on Sine and Tent systems is proposed. Also in the encryption algorithm, 3D shift based on chaotic system is introduced. The simulation results and security analysis show that the proposed algorithm is secure and efficient.

Keywords: Encryption; Compression; Chaotic system; Fuzzy transform; B-spline.

1 Introduction

In recent years with the development of the information transmission, fast and secure transmission have become important subject. Various type of methods for compression-encryption and encryption have been studied in [1, 2, 3, 4, 5, 6]. Also multi- image encryption have been studied in [7, 8]. In this work, in the first step we use the fuzzy transform for image compression step. Lossy image compression and reconstruction basis on fuzzy transform has been proposed in [9, 10, 11]. For fuzzy partition in fuzzy transform method, exponential b-spline function is used, more details about this function can be found in [12, 13]. In the next step, for encryption algorithm, a combination chaotic system is introduced. This system is introduced in [14]. In this system for all values of $r \in (0, 4]$ the Lyapunov exponent is positive. Also the combination

*zarebnia@uma.ac.ir

†rahele.kianfar@student.uma.ac.ir

‡Corresponding author: rparvaz@uma.ac.ir

chaotic system have uniform distribution over output range. In the encryption algorithm, by using chaotic system, we define two-dimensional block matrix shift and three-dimensional matrix shift. Then by using these matrices, images are scrambled.

The organization of this paper is as follows: In Section 2, image compression and reconstruction by using fuzzy transform is explained. In Section 3, we introduce the chaotic system and the color image encryption algorithm. Experimental results and algorithm analysis are given in Section 4. A summary is given at the end of the paper in Section 5.

2 Fuzzy transform based on exponential b-spline

In this section, we describe fuzzy transform based on exponential b-spline. The basis of exponential b-spline has been proposed in [12, 13]. For non-decreasing sequence of knots as $x_1 \leq x_2 \leq \dots \leq x_n$, exponential B-splines of order 2 are defined as follows

$$B_0^2(x) := \begin{cases} \frac{\sinh(\rho_1(x_2-x))}{\sinh(\rho_1 h_1)}, & x \in [x_1, x_2], \\ 0, & \textit{otherwise}, \end{cases} \quad (2.1)$$

$$B_n^2(x) := \begin{cases} \frac{\sinh(\rho_{n-1}(x-x_{n-1}))}{\sinh(\rho_{n-1} h_{n-1})}, & x \in [x_{n-1}, x_n], \\ 0, & \textit{otherwise}. \end{cases} \quad (2.2)$$

Also for $i = 1, \dots, n-1$, we define

$$B_i^2(x) := \begin{cases} \frac{\sinh(\rho_{i-1}(x-x_{i-1}))}{\sinh(\rho_{i-1} h_{i-1})}, & x \in [x_{i-1}, x_i], \\ \frac{\sinh(\rho_i(x_{i+1}-x))}{\sinh(\rho_i h_i)}, & x \in [x_i, x_{i+1}], \\ 0, & \textit{otherwise}, \end{cases} \quad (2.3)$$

where ρ_i ($i = 1, \dots, n-1$) are tension parameters and $h_i := x_{i+1} - x_i$. The tension parameter in b-spline function plays a important role in the slope of the function (see Fig.1). Also exponential B-splines of arbitrary order can be found as follows

$$B_j^k(x) := \frac{\int_{x_j}^x B_j^{k-1}(y)dy}{\sigma_j^{k-1}} - \frac{\int_{x_{j+1}}^x B_{j+1}^{k-1}(y)dy}{\sigma_{j+1}^{k-1}}, \quad k = 3, 4, \dots,$$

where

$$\sigma_j^{k-1} := \int_{x_j}^{x_{j+k-1}} B_j^{k-1}(y)dy.$$

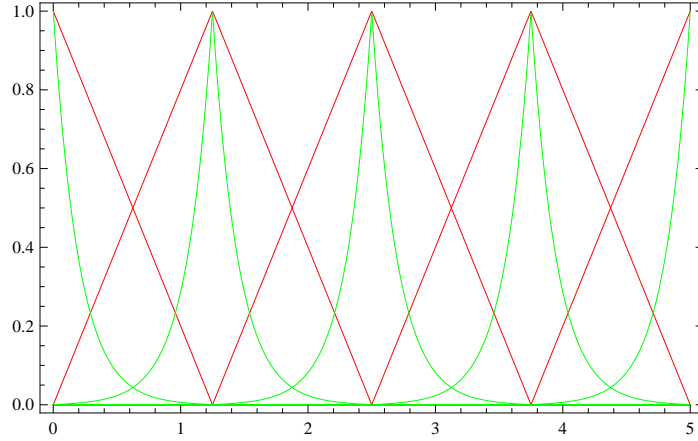


Figure 1: Comparisons between exponential b-spline for different values of tension parameters, red lines for $\rho_i = 0.001$ and green lines for $\rho_i = 5$, ($i = 1, \dots, 5$).

The first study in fuzzy transform is introduced by Irina Perfilieva [9]. According to [9], Fuzzy partition and F-transforms (Fuzzy transforms) are defined as follows.

Definition 2.1. [9] Let $a = x_1 < \dots < x_n = b$, ($n \geq 2$) be fixed nodes within $[a, b]$. We say that fuzzy sets A_1, \dots, A_n , identified with their membership functions $A_1(x), \dots, A_n(x)$, defined on $[a, b]$, form a fuzzy partition of $[a, b]$, if the fulfill the following conditions for $k = 1, \dots, n$:

$$1-A_k[a, b] \longrightarrow [0, 1], A_k(x_k) = 1;$$

$$2-A_k(x) = 0 \text{ if } x \notin (x_{k-1}, x_{k+1});$$

3- A_k is continuous;

4- $A_k, k = 2, \dots, n$, strictly increases on $[x_{k-1}, x_k]$ and $A_k, k = 1, \dots, n-1$, strictly decreases on $[x_k, x_{k+1}]$

$$5\text{-for all } x \in [a, b], \sum_{k=1}^n A_k(x) = 1.$$

For a function f be given at nodes $(p_i, q_i) \in [a, b] \times [c, d]$, $i = 1, \dots, N$, $j = 1, \dots, M$, discrete F-transform is defined as

$$F_{kl} = \frac{\sum_{j=1}^M \sum_{i=1}^N f_i(p_i, q_j) A_k(p_i) C_l(q_j)}{\sum_{j=1}^M \sum_{i=1}^N A_k(p_i) C_l(q_j)}, \quad k = 1, \dots, n, \quad l = 1, \dots, m, \quad (2.4)$$

where $A_1, \dots, A_n, C_1, \dots, C_m$ ($n < N, m < M$) are fuzzy partitions of $[a, b]$ and $[c, d]$, respectively. Also the inverse of F -transform is defined as

$$f_{nm}^F(x, y) = \sum_{k=1}^n \sum_{l=1}^m F_{kl} A_k(x) C_l(y). \quad (2.5)$$

We can easily prove that $\{B_i^2\}_i^n$ is satisfied in the Definition 2.1. In compression step we consider B_i^2 as A_i and C_i , then we use fuzzy transform for image compression.

3 Construction of the algorithm

3.1 Compression-encryption algorithm

It is known that the histogram of the Logistic Tent system is not flat enough. For solving this problem we add weights and functions in the Logistic Tent system or the Sine Tent system. For details, the reader can see [14]. In this paper we consider a combination chaotic system based on Sine and Tent systems as follows

$$X_{n+1} := \begin{cases} \omega_1 f_1 \circ F(r, X_n) + \alpha_1 g_1(rX_n) + \xi_1 \frac{(\beta_1 - r)X_n}{2} \bmod 1, & \text{when } X_n < 0.5, \\ \omega_2 f_2 \circ F(r, X_n) + \alpha_2 g_2(rX_n) + \xi_2 \frac{(\beta_2 - r)(1 - X_n)}{2} \bmod 1, & \text{when } X_n \geq 0.5, \end{cases} \quad (3.1)$$

where $\omega_1 = \omega_2 = 1, \alpha_1 = \alpha_2 = 1, \xi_1 = 7, \xi_2 = 15, \beta_1 = 40, \beta_2 = 20, f_1 = \cos, f_2 = \tan, g_1 = \tan, g_2 = x, F(r, x_n) = r \sin(\pi x_n)/4$. The Lyapunov exponent, Bifurcation, Histogram and Cobweb plots of combination chaotic system are given in figure 3.1. From this figure we can see that for all values of r , the Lyapunov exponent is positive. The Cobweb plots show chaotic behavior. Also this figure show that the chaotic system has uniform distribution over output range. The following definitions are used in proposed algorithm.

Definition 3.1. For an arbitrary vector $w \in R^{nm}$, matrix $\Delta(w) = (\delta_{i,j}) \in R^{n \times m}$ is defined as follows

$$\delta(i, j) := w(i + (j - 1)n), \quad i = 1, \dots, n, \quad j = 1, \dots, m.$$

Definition 3.2. For an arbitrary vector $w \in R^{3nm}$, matrix $\Lambda(w) = (\lambda_{i,j,l}) \in R^{n \times m \times 3}$ is defined as follows

$$\lambda(i, j, l) := w(i + (j - 1)n + (l - 1)nm), \quad i = 1, \dots, n, \quad j = 1, \dots, m, \quad l = 1, 2, 3.$$

Definition 3.3. Consider matrix $A = (a_{i,j}) \in R^{n \times m}$ such that for all (i, j) and (k, l) with $(i, j) \neq (k, l)$, we have $a_{i,j} \neq a_{k,l}$. Suppose matrix $B = (b_{i,j}) \in R^{n \times m}$ that for all (i, j) , $b_{i,j} = a_{k,l}$ for some (k, l) . For a block matrix $C = (C_{i,j})$ we define a block matrix $\Upsilon_{A \rightarrow B}^2(C) = (D_{i,j})$, where $D_{i,j} = C_{k,l}$.

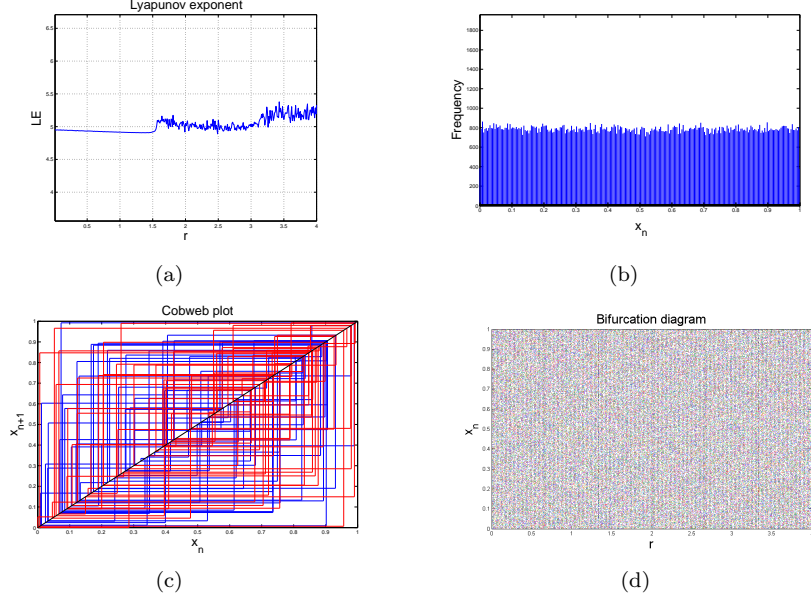


Figure 2: (a) Lyapunov exponent plot, (b) Histogram plot, (c) Cobweb plot, (d) Bifurcation diagram.

Definition 3.4. Consider matrix $A = (a_{i,j,l}) \in R^{n \times m \times 3}$ such that for all (i, j, d) and (k, l, s) with $(i, j, d) \neq (k, l, s)$, we have $a_{i,j,d} \neq a_{k,l,s}$. Suppose matrix $B = (b_{i,j,d}) \in R^{n \times m \times 3}$ that for all (i, j, d) , $b_{i,j,d} = a_{k,l,s}$ for some (k, l, s) . For a matrix $C = (c_{i,j,k})$ we define a matrix $\Upsilon_{A \rightarrow B}^2(C) = (d_{i,j,k})$, where $d_{i,j,k} = c_{k,l,s}$.

For above definitions we can say that

$$\Upsilon_{B \rightarrow A}^l(\Upsilon_{A \rightarrow B}^l(C)) = \Upsilon_{A \rightarrow B}^l(\Upsilon_{B \rightarrow A}^l(C)) = C, \quad l = 2, 3.$$

In this section we assume that we have a set of N images as I^1, \dots, I^N . Also let the size of all the images are $n \times m \times 3$. In the following algorithm $\mu(x_0, r, n)$ represents a vector as (x_1, \dots, x_n) where $x_i (i = 1, \dots, n)$ are defined by using (3.1) with x_0 . The compression-encryption algorithm is written in the following steps.

Step 1. In the first step input images are converted into R(red), G(green), B(blue) component matrix. Then we use exponential b-spline fuzzy transform for each component part. We assume that the size of compressed image is $nc \times mc \times 3$. In this step compressed images are considered as $CI^i (i = 1, \dots, N)$.

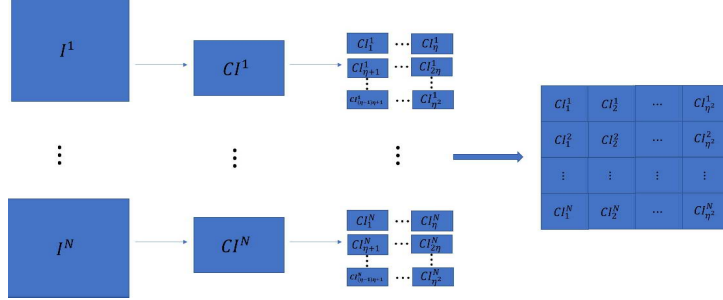


Figure 3: The step 1 and step 2 process of the proposed algorithm.

Step 2. For $i = 1, \dots, N$, CI^i is divided into η^2 parts as CI_j^i ($i = 1, \dots, N$, $j = 1, \dots, \eta^2$), where

$$\eta := \begin{cases} 2, & \text{when } N \text{ is } 1, 2 \text{ or } 3, \\ \lfloor \sqrt{N} \rfloor, & \text{otherwise.} \end{cases} \quad (3.2)$$

Then we consider a block matrix as $\Theta = (CI_j^i)$ (see figure 3.1).

Step 3.

- a) v^l ($l = 1, 2, 3$) are defined as $v^l = \mu(x_0^l, r_l, N\eta^2)$ with $x_0^l := \frac{\sum_{i,j} CI^i(:, :, l)}{nc \times mc \times 255}$ ($l = 1, 2, 3$).
- b) $Sv^l := \text{sort}(v^l)$ ($l = 1, 2, 3$) (smallest to largest).
- c) A^l and P^l are considered as $A^l = \Delta(V^l)$, $P^l = \Delta(SV^l)$ ($l = 1, 2, 3$).
- d) C is defined as $C(:, :, l) := \Upsilon_{A^l \rightarrow P^l}^2(\Theta(:, :, l))$ ($l = 1, 2, 3$).

Step 4.

- a) To generate different keys in each iteration, we consider x^0 as random number in $(0, 1)$ then we define v^0 as $\mu(x_0^0, r_0, N \times nc \times mc)$.
- b) $Sv^0 := \text{sort}(v^0)$ (smallest to largest).
- c) Consider $A^0 = \Lambda(v^0)$, $P^0 = \Lambda(Sv^0)$.

d) By using *xor* operation and $\Upsilon_{A^0 \rightarrow P^0}^3$, matrix EI is determined by

$$EI := \Upsilon_{A^0 \rightarrow P^0}^3(C) \oplus A.$$

e) The final encrypted image is found as follows

$$EI = \text{circshift}(EI, [\rho_1 \ \rho_2 \ \rho_2]),$$

where $\text{circshift}(A, r)$ circularly shifts the values in array A by r positions and $\rho_l = \lfloor x_l \times 10^2 \rfloor$, $l = 1, 2, 3$.

3.2 Decryption algorithm

The decryption algorithm is the inverse process of the encryption algorithm. In the first step by using Algorithm 1, compressed images are found. Then by using inverse of the F-transform we can find images.

Algorithm 1: Decryption Algorithm

Input : $EI_{N \times nc \times mc}$ (Compression-encryption image),
 $\{x_i\}_{i=0}^3, \{r_i\}_{i=0}^3$ (Keys),
Output: $\{CI^i\}_{i=1}^N$ (Compressed images),
1 **for** $l=1:3$ **do**
2 $V^l := \mu(x_l, r_l, N\eta^2)$;
3 $A^l := \Delta(V^l), P^l := \Delta(\text{sort}(V^l))$;
4 $\rho_l = \lfloor x_l \times 10^2 \rfloor$;
5 **end**
6 $V^0 := \mu(x_0, r_0, N \times nc \times mc)$;
7 $A^0 := \Lambda(V^0), P^0 := \Lambda(\text{sort}(V^0))$;
8 $EI = \text{circshift}(EI, [\rho_1 \ \rho_2 \ \rho_3])$;
9 $C = \Upsilon_{P^0 \rightarrow A^0}^3(EI) \oplus A$;
10 **for** $l=1:3$ **do**
11 $\Theta(:, :, l) := \Upsilon_{P^l \rightarrow A^l}^2(C(:, :, l))$;
12 **end**

4 Experimental results and security analysis

4.1 Experimental results

In this section, as plain images, we use color images ‘‘Baboon, Lena, Peppers and House’’ (the 256×256 images with 256 grey levels) as I^1, I^2, I^3 and I^4 respectively. In compression step 0.1 is used as tension parameter. Also we consider $nc = mc = 100$. Fig. 4 shows original images and compressed images by using exponential b-spline fuzzy transform. Also simulation results for encryption algorithm are shown in Fig. 5. In this section, we consider the secret keys as $r_0 = 3.02, r_1 = r_2 = r_3 = 2$. Also for simulation results, we use Matlab R2014b programming.

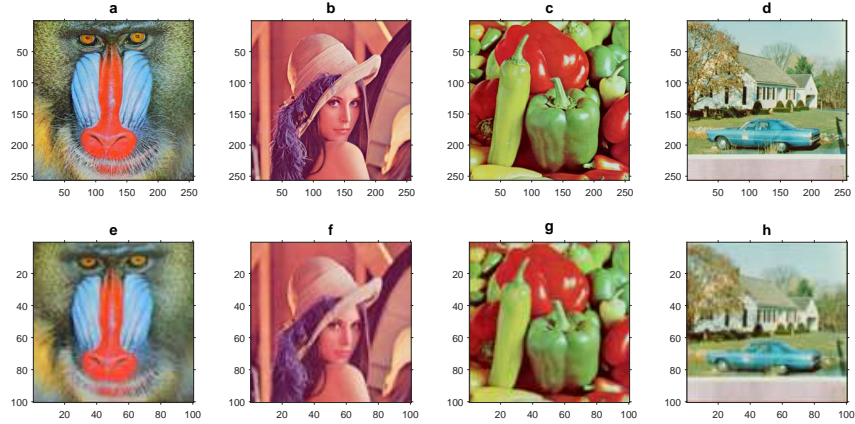


Figure 4: (a-b-c-d) Original images, (e-f-g-h) Compressed images.

4.2 Key analysis

In the encryption algorithm, the security keys of the proposed algorithm are composed of eight parameters. In the image encryption algorithm, if we use 10^{15} as the precision, the key space is almost 10^{120} , and this space is sufficiently large to resist the brute force attack [15]. In the next step, we study key sensitivity. We change r_0 as $r_0 = 3.02 + 10^{-15}$. Fig. 6. shows decryption images by using changed key. By using this figure, we can see that the original images cannot be reconstructed. Then, we can see that the proposed algorithm has high key sensitivity. Also in Step 4 of encryption algorithm, a random number is used as encryption key. Therefore we can generate different keys in each iteration. We run the encryption algorithm twice and by using pixel-to-pixel the difference between the two images are illustrate in Fig. 7. It can be seen in Fig. 7, two encrypted images are different. Therefore the proposed algorithm is able to resist the chosen-plain text attack.

4.3 Noise and Data loss attacks

Appropriate encryption algorithm should resist the data loss and noise attacks. In the data loss attack, some image data disappears. To simulate this attack, in

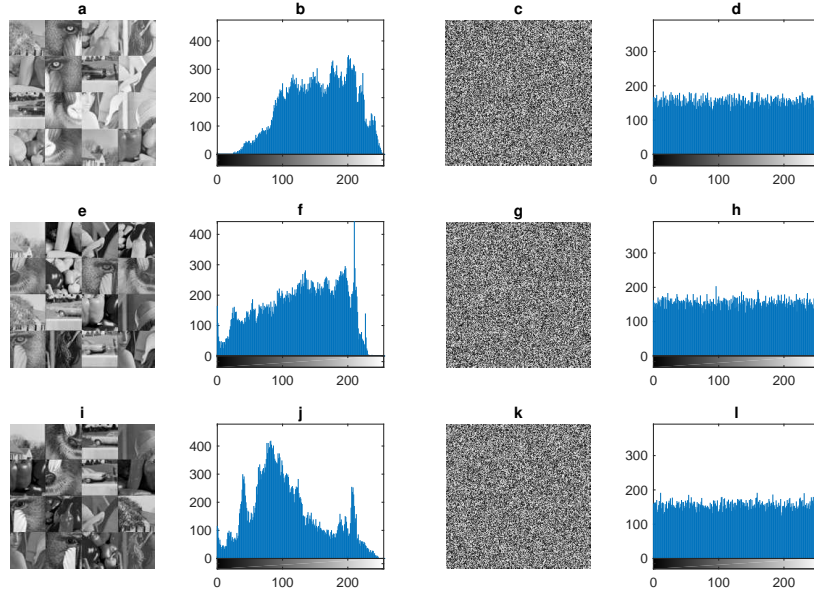


Figure 5: (a-e-i) R, G, B components of the step 2 process of the proposed algorithm, (b-f-j) Histograms of R, G, B components of the step 2 process of the proposed algorithm, (c-g-k), R, G, B components of the encrypted image, (d-h-l) Histograms of R, G, B components of the encrypted image.

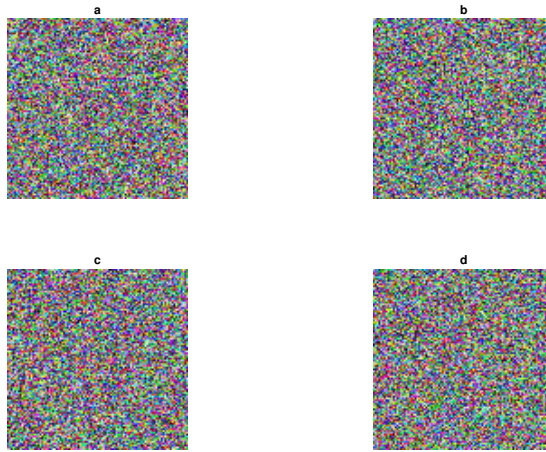


Figure 6: Decrypted images by using changed key.

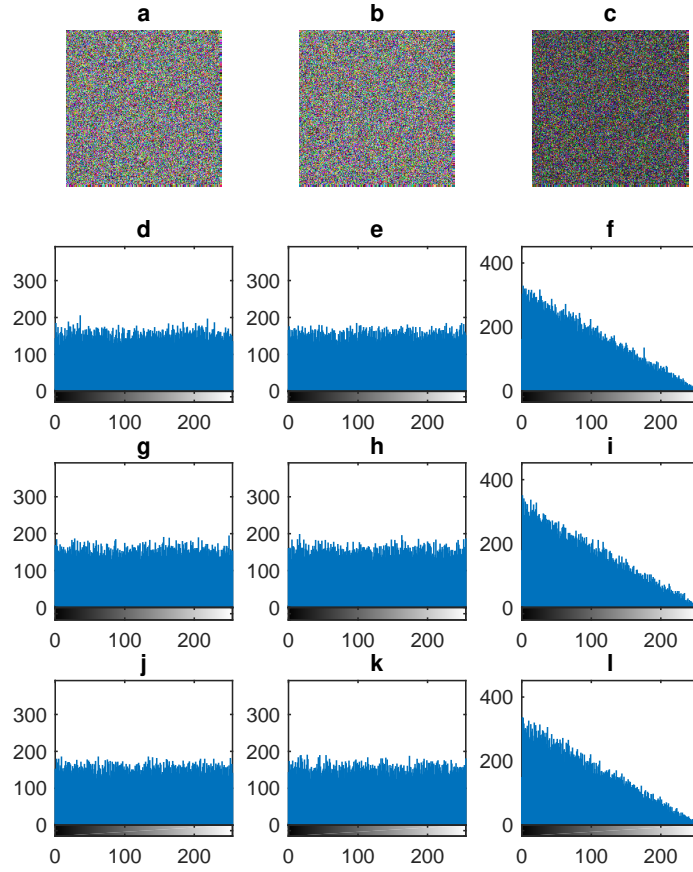


Figure 7: (a-d-g-j) The first encrypted image and histogram of R, G, B components, (b-e-h-k) The second encrypted image and histogram of R, G, B components, (c-f-i-l) The pixel-to-pixel difference and histogram of R, G, B components.

Fig. 8, we remove 100×100 of encrypted image. Also in the noise attack, noise is added to the encrypted image. An appropriate encryption algorithm should not increase the amount of these noises. To simulate noise attack, Gaussian noise with zero-mean and $var = 0.2$ is added to encrypted image. The simulation results are given in Figs 8-9. In these figures we can see that the reconstructed images contain most of original visual in formation and we can recognize the original images.

4.4 Statistical analysis

Some statistical analysis as correlation values, information entropy are studied in this section. In the appropriate encryption algorithm, the correlation values between adjacent pixels are close to zero. The correlation coefficients of adjacent pixels in the plain images and encrypted images are given in Table 1 and Figs 10-11. By using numerical results, we can say that the correlation coefficients of plain images are close to one, and the correlation coefficients of the encrypted image are close to zero. The correlation values are found by using formula [16]

$$C_{xy} = \frac{E[(x - \mu_x)(y - \mu_y)]}{\sigma_x \sigma_y}, \quad (4.1)$$

where $E[\cdot]$ denotes the expectation value, μ is the mean value and σ represents standard deviation.

In the next step we study histogram analysis. The evaluation of the robustness of an encrypted image is studied by using histogram analysis. The histograms of ciphered image are shown in Fig. 5. The histograms show that distribution of pixel values in the encrypted image is close to uniform distribution. Also chi-square test outputs are given in Table 2. By using chi-square test, we accept that the data have a uniform distribution at level 0.05. Also unpredictability of information can be studied by using unpredictability of information the information entropy. The information entropy is defined as follows [17]

$$H(k) = - \sum_{i=0}^{w-1} P(k_i) \log_2 P(k_i), \quad (4.2)$$

where w is the gray level and $P(\cdot)$ denotes the probability of symbol. The ideal value of the information entropy is 8. Numerical results for the information entropy are given in Table 3. From Table 3, we can say that results for the encryption algorithm are very close to the ideal value. From the above discussion, we can conclude that the proposed algorithm has stronger ability to withstand statistical attacks.

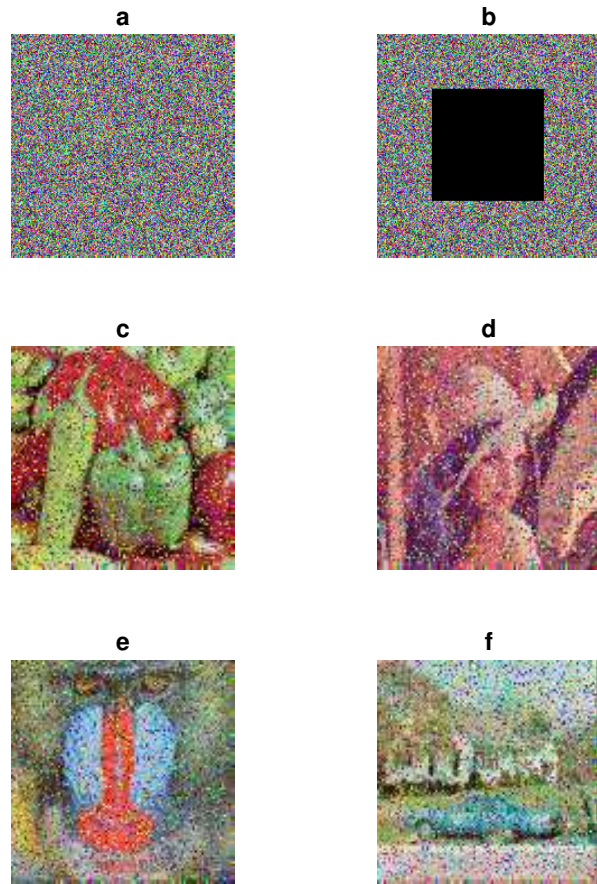


Figure 8: (a) Encrypted image, (b) Cropped attack image, (c-d-e-f) Decryption results.

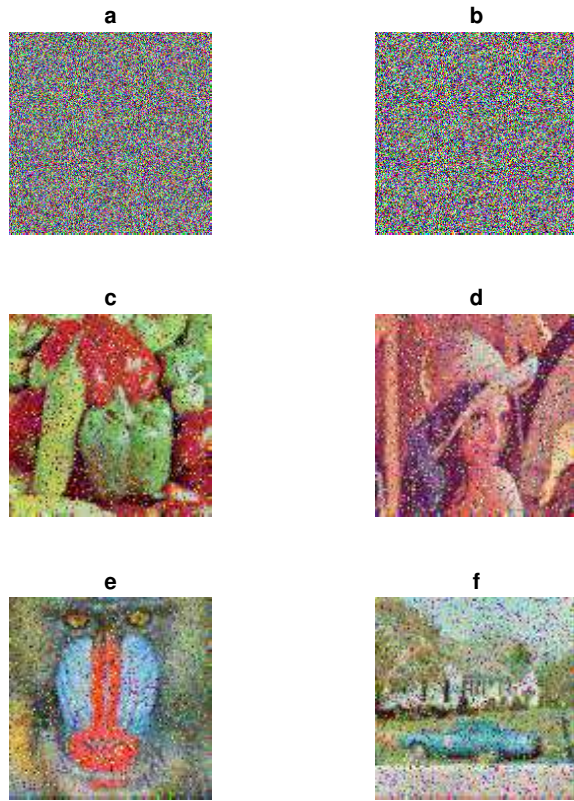


Figure 9: (a) Encrypted image, (b) Noise attack image with $\text{var}=0.2$, (c-d-e-f) Decryption results.

Table 1: Correlation coefficient values in the plain images and the cipher image.

Image	Component	Horizontal	Vertical	Diagonal	Diagonal
				(lower left to top right)	(lower right to top left)
Baboon	R	0.9635	0.9663	0.9585	0.9564
	G	0.9811	0.9818	0.9709	0.9687
	B	0.9665	0.9664	0.9478	0.9478
Lena	R	0.9798	0.9893	0.9777	0.9697
	G	0.9691	0.9825	0.9654	0.9555
	B	0.9327	0.9576	0.9254	0.9183
Peppers	R	0.9231	0.8660	0.8519	0.8543
	G	0.8655	0.7650	0.7249	0.7348
	B	0.9073	0.8809	0.8424	0.8399
House	R	0.9536	0.9579	0.9240	0.9224
	G	0.9391	0.9423	0.8940	0.8901
	B	0.9725	0.9686	0.9459	0.9445
Ciphered image	R	0.0070	0.0025	-0.0066	-0.0014
	G	0.0019	0.0072	0.0030	0.0056
	B	-0.0004	0.0019	0.0048	0.0008

Table 2: Chi-square outputs for ciphered image.

	R Component	G Component	B Component
Chi-square statistics	236.6	288.1	240.5
df	255	255	255
p-value	0.790	0.076	0.735

Table 3: Information entropy, NPCR and UACI results.

	Information entropy	NPCR	UACI
R Component	7.9955	99.6250	33.4561
G Component	7.9945	99.6400	33.4212
B Component	7.9952	99.6250	33.3425

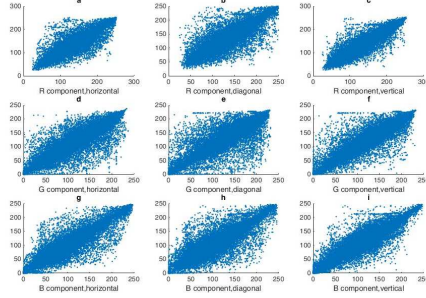


Figure 10: Correlation of neighbourhood pixels at different directions of Θ .

4.5 Sensitivity analysis

NPCR (number of pixels change rate) and UACI (unified average change intensity) are calculated as

$$NPCR = \frac{\sum_{i,j} D(i,j)}{m \times n} \times 100\%, \quad (4.3)$$

$$UACI = \frac{1}{m \times n} \left[\frac{\sum_{i,j} |C_1(i,j) - C_2(i,j)|}{255} \right] \times 100\%, \quad (4.4)$$

where

$$D(i,j) := \begin{cases} 1, & \text{when } C_1(i,j) \neq C_2(i,j), \\ 0, & \text{when } C_1(i,j) = C_2(i,j). \end{cases} \quad (4.5)$$

In above formulae, $C_1(i,j)$ and $C_2(i,j)$ are denoted the cipher image before and after one pixel of the plain image is changed. The sensitive to the changing of plain image can be studied using NPCR and UACI. The best value for NPCR is 100%. Also the ideal value for UACI is $33.\overline{33}\%$. In this step, $I_1(10, 50, 2)$, $I_2(20, 30, 3)$, $I_3(60, 35, 1)$ and $I_4(75, 34, 2)$ are changed to 0. The simulation results in Table 3 are close to ideal values. Therefore, we can say that the differential attack is impossible on proposed algorithm.

5 Conclusion

In this paper, by using fuzzy transform and combination chaotic system, we have introduced a multi-color image compression-encryption algorithm. In fuzzy

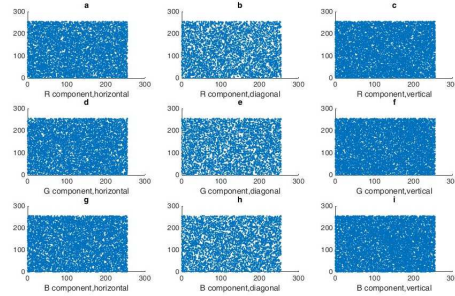


Figure 11: Correlation of neighbourhood pixels at different directions of the encrypted image.

transform, exponential b-spline function is used as fuzzy partition. Simulation results shown that the proposed encryption algorithm can effectively resist differential, statistical, noise, data loss, chosen-plain text attacks.

References

- [1] A. Kanso, M. Ghebleh. *An algorithm for encryption of secret images into meaningful images*. Optics and Lasers in Engineering 90 (2017): 196-208.
- [2] N. Zhou, A. Zhang, F. Zheng, L. Gong. *Novel image compression encryption hybrid algorithm based on key-controlled measurement matrix in compressive sensing*. Optics & Laser Technology 62 (2014): 152-160.
- [3] Z. Li, X. Sun, Q. Ding. *Design and implementation in image compression encryption of digital chaos based on matlab*. In Intelligent Data analysis and its Applications, Volume II, pp. 509-518. Springer, Cham, 2014.
- [4] N. Jindal, K. Singh. *Joint image compression encryption using discrete fractional transforms*. The Imaging Science Journal 62, no. 5 (2014): 265-272.
- [5] Zhang, Liguo, Binghang He, Jianguo Sun, Mingzhu Lai, and Zhihan Lv. "Double image multi-encryption algorithm based on fractional chaotic time series." Journal of Computational and Theoretical Nanoscience 12, no. 11 (2015): 4980-4986.
- [6] Ü. Çavuşoğlu, S. Kaçar, I. Pehlivan, A. Zengina, *Secure image encryption algorithm design using a novel chaos based S-Box*, Chaos, Solitons & Fractals 95 (2017) 92-101.

- [7] D. Kong, X. Shen, Y. Shen, Xin Wang. *Multi-image encryption based on interference of computer generated hologram*. Optik-International Journal for Light and Electron Optics 125, no. 10 (2014): 2365-2368.
- [8] S. Banerjee, S. Mukhopadhyay, L. Rondoni. *Multi-image encryption based on synchronization of chaotic lasers and iris authentication*. Optics and Lasers in Engineering 50.7 (2012): 950-957.
- [9] I. Perfilieva. *Fuzzy transforms: Theory and applications*. Fuzzy sets and systems 157, no. 8 (2006): 993-1023.
- [10] F.D. Martino, V. Loia, I. Perfilieva, S. Sessa. *An image coding/decoding method based on direct and inverse fuzzy transforms*. International Journal of Approximate Reasoning 48, no. 1 (2008): 110-131.
- [11] I. Perfilieva, V. Novék, A. Dvořák. *Fuzzy transform in the analysis of data*. International Journal of Approximate Reasoning 48, no. 1 (2008): 36-46.
- [12] P.E. Koch, T. Lyche. *Interpolation with exponential B-splines in tension*. In Geometric modelling, pp. 173-190. Springer, Vienna, 1993.
- [13] I. Beroš, M. Marušić. *Evaluation of tension splines*. Mathematical Communications 4, no. 1 (1999): 73-81..
- [14] R. Parvaz, M. Zarebnia. *A combination chaotic system and application in color image encryption*. arXiv:1708.01862.
- [15] G. Alvarez, S. Li. *Some basic cryptographic requirements for chaos-based cryptosystems*. Int J Bifurcation Chaos 2006;16(8):212951.
- [16] N. Zheng, J. Xue. *Statistical learning and pattern analysis for image and video processing*. Springer Science & Business Media, 2009.
- [17] F.A El-Samie, H.H. Ahmed, I.F. Elashry, M.H. Shahieen, O.S. Faragalah, E.M. El-Rabaie, S.A. Alshebeili. *Image Encryption: A Communication Perspective*. CRC Press 2014.